Electronic Supplementary Information

Freestanding Single-Crystal $Ni_{0.5}Zn_{0.5}Fe_2O_4$ Ferrite Membranes with Controllable Enhanced Magnetic Properties for Flexible RF/microwave Applications

Mouteng Yao[1, †], Yaojin Li[1, †], Bian Tian[2, †], Qi Mao[2], Guohua Dong[1], Yuxin Cheng[1], Weixiao Hou[1], Yanan Zhao[1], Tian Wang[1], Yifan Zhao[1], Zhuangde Jiang[2], Ming Liu[1], Ziyao Zhou[1, *]

1. Ministry Education Key Laboratory of Electronic Materials Research Laboratory, School of Electronic Science and Engineering, State Key Laboratory for Mechanical Behavior of Materials, the International Joint Laboratory for Micro/Nano Manufacturing and Measurement Technology, Xi'an Jiaotong University, Xi'an 710049, China.
2. State Key Laboratory for Mechanical Manufacturing Systems Engineering, International Joint Laboratory for Micro/Nano Manufacturing and Measurement Technology, School of Mechanical Engineering, Xi'an Jiaotong University, Xi'an 710049, China.

† These authors contribute equally.

* Corresponding author.

E-mail: ziyaozhou@xjtu.edu.cn

Supplementary Figures

Figure S1 (a) and (b) show the topographic AFM image of as-grown NZFO film and transferred NZFO film on a silicon wafer, respectively. The thickness of NZFO is ~ 120 nm obtained from Figure S1 (b).

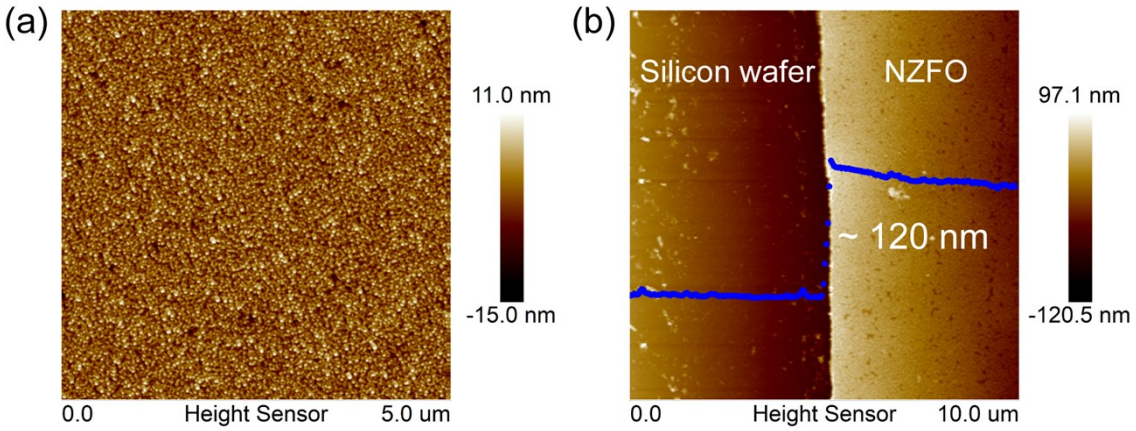

Figure S1 Topographic AFM image of as-grown NZFO film (a) and transferred NZFO film on a silicon wafer (b).

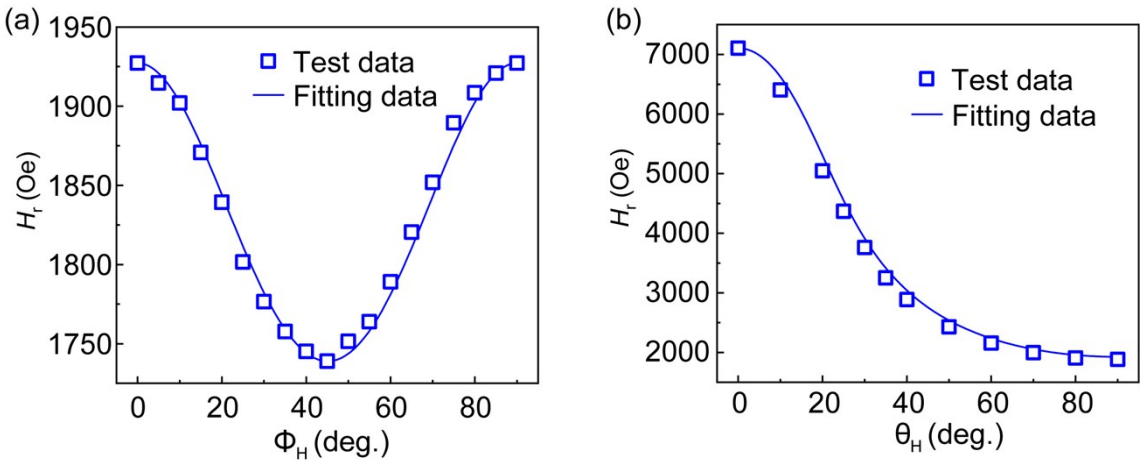

Figure S2 H_r as a function of in-plane field orientation Φ_H (a) and out-of-plane inclination angle θ_H (b) for as-grown NZFO film.

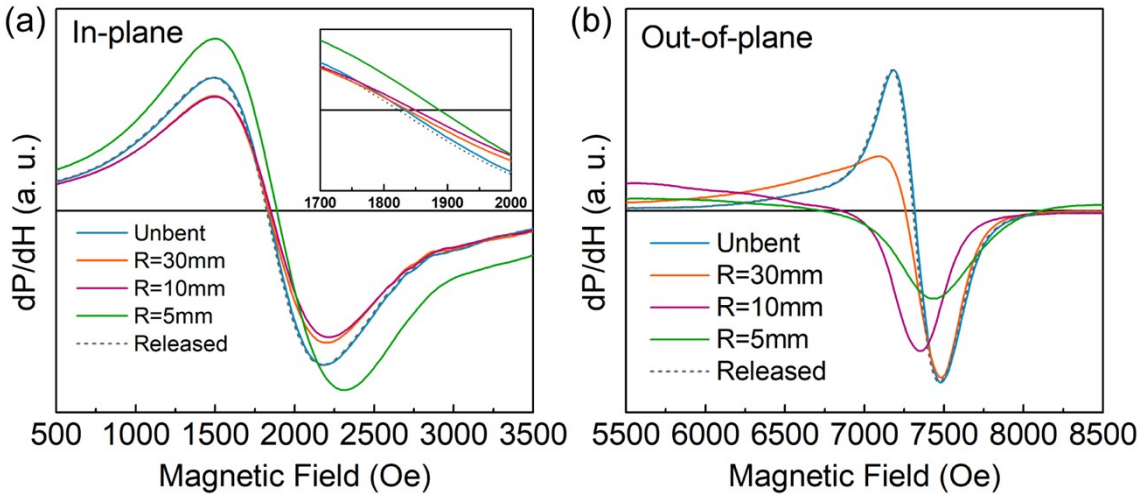

Figure S3 The FMR spectra of transferred NZFO film in the state of compressive strain along in-plane (a) and out-of-plane (b) directions with a various radius of curvatures.

For the purpose of the application, the antifatigue of flexible thin films is one of the most significant characters. The in-plane, TMS critical angle and out-of-plane FMR fields of the flexible NZFO thin-film almost keep unchanged for the fatigue cycle up to 20000 times, as shown in Figure S4 (a), (b) and (c). The FMR fields and the change of FMR fields as a function of cycles are shown in Figure S4 (d) and (e).

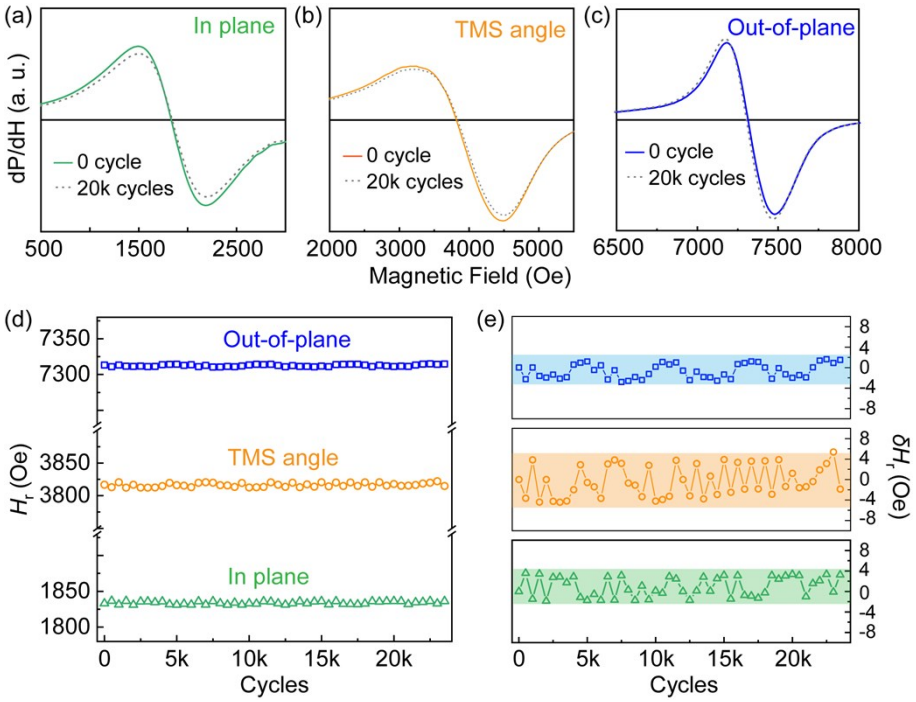

Figure S4 Fatigue character for the NZFO flexible in unbent and bent for 20 000 cycles, respectively. FMR spectra for in-plane (a), TMS angle (b) and out-of-plane (c). FMR field and the change of FMR field (e) as a function of cycles for in-plane, TMS angle, and out-of-plane, respectively.

Figure S5 (c) shows the magnetic hysteresis loops of flexible NZFO film with various radius of curvatures in the state of tensile strain, and it can be clearly observed that saturation magnetization gradually decreases with the radius of curvatures decrease. Before the VSM test, the system was calibrated, and we define the surface of the unbent sample as the datum plane, as shown in Figure S5 (a-II). For the bending test, the flexible NZFO film was attached to the holders with various radius of curvatures. And the thickness of holders is 1.2 mm, 1.6 mm, and 2.0 mm, respectively, as shown in Figure S5 (a-I). Thus, the maximum distance (D) between the surface of the film and the datum plane gradually increases due to the thickness of the holders for the VSM test are different, leading to the inhomogeneous distribution of the test magnetic field. We surmise that the reduction of saturation magnetization might come from the inhomogeneous distribution of the test magnetic field and be independent of the magnitude of strain. Figure S5 (b) shows the ΔM as a function of D/L of transferred NZFO film in the state of tensile strain.

In order to exclude the strain effect, the unbent sample was measured when D is 1.2 mm, 1.6 mm, and 2.0 mm, respectively. Figure S5 (e) presents the magnetic hysteresis loops of unbent flexible NZFO film, and it can be distinctly seen that saturation magnetization also decreases with the value

of D increases. This further suggests that the reduction of saturation magnetization is independent of the magnitude of strain.

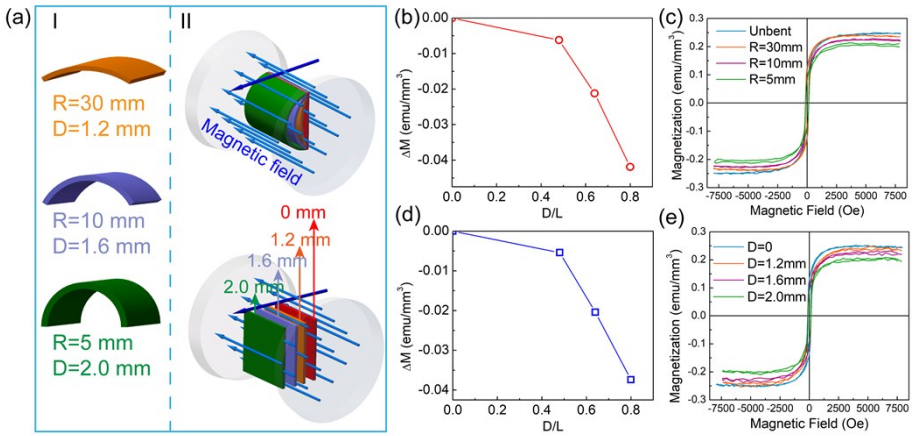

Figure S5 (a) Schematic of the holder with a different radius (I) and VSM test conditions (II). (b) ΔM as a function of D/L of flexible NZFO film in the state of tensile strain. (c) Magnetic hysteresis loops of transferred NZFO film. (d) ΔM as a function of D/L of transferred NZFO film. (e) Magnetic hysteresis loops of flexible NZFO film.

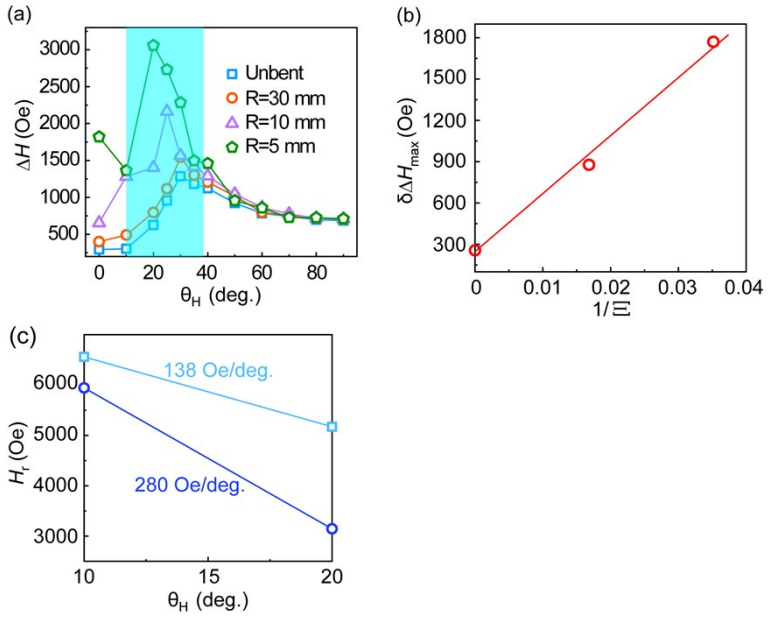

Figure S6 (a) The ΔH as a function of θ_H for various R. (b) The $\delta\Delta H_{max}$ as a function of $\delta 1/\Xi$. Ξ is the magnetic dragging function. (c) The enlarged view of Figure 5 (a).

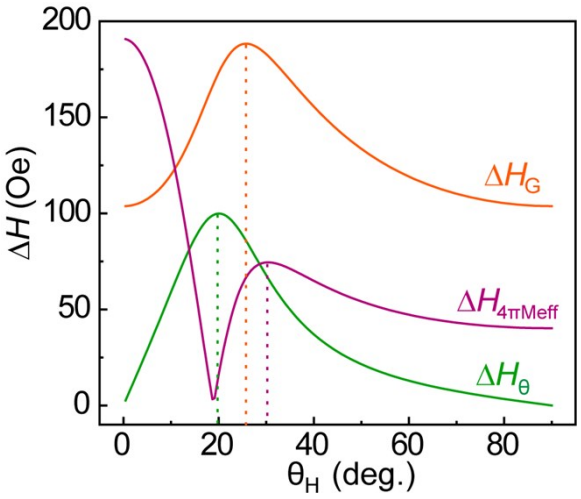

Figure S7 Enlarge view of Figure 4 (b).

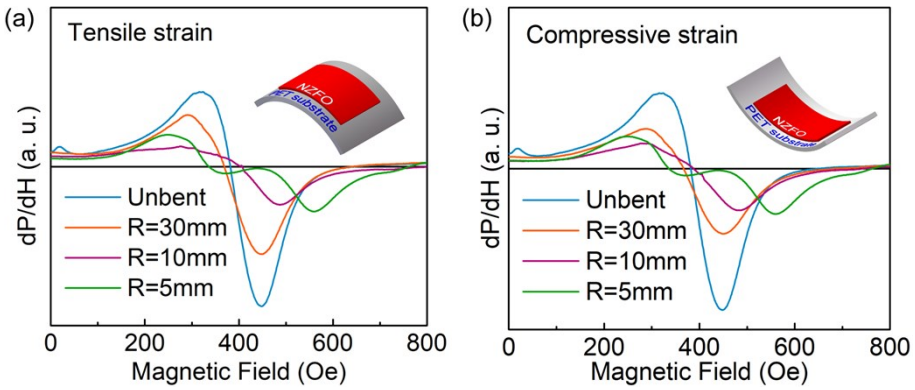

Figure S8 The FMR spectra at TMS critical angle of transferred NZFO films (a) in the state of tensile strain and (b) in the state of compressive strain.

Table S1 The values of $H_{4\perp}$, $H_{4//}$, M_{eff} and $H_{2//}$ for as-grown and transferred NZFO films

	f	$H_{4\perp}$	$H_{4//}$	M_{eff}	$H_{2//}$
STO	9.4 GHz	326.28 Oe	-56.87 Oe	350.26 Oe	0 Oe
PET	9.4 GHz	404.44 Oe	-56.07 Oe	379.74 Oe	7 Oe

Formula derivation

Smit-Beljer's approach Equation (S1).

$$\left(\frac{2\pi f}{\gamma}\right)^2 = \frac{1}{M^2 Sin^2\theta}\left[\frac{\partial^2 F}{\partial\theta^2}\frac{\partial^2 F}{\partial\Phi^2} - \left(\frac{\partial^2 F}{\partial\theta\partial\Phi}\right)^2\right] \quad \text{(S1)}$$

$$\left(\frac{2\pi f}{\gamma}\right)^2 = H_X H_Y \quad \text{(S2)}$$

$$H_X = H_r(Cos\theta Cos\theta_H + Cos(\Phi - \Phi_H)Sin\theta Sin\theta_H) - 4\pi M_{eff}Cos^2\theta + 2H_{4\perp}Cos^4\theta$$
$$- \frac{1}{4}H_{4//}\left[6Cos^2\theta + (Cos2\theta - 7)Cos4\Phi\right]Sin^2\theta + H_{2//}[Cos^2\theta Sin^2\Phi + Cos2\Phi] \quad \text{(S2-1)}$$

$$H_Y = H_r(Cos\theta Cos\theta_H + Cos(\Phi - \Phi_H)Sin\theta Sin\theta_H) - 4\pi M_{eff}Cos2\theta + H_{4\perp}(Cos4\theta + Cos2\theta) +$$
$$\frac{1}{4}H_{4//}(3 + Cos4\Phi)(Cos4\theta - Cos2\theta) + H_{2//}Cos2\theta Sin^2\Phi \quad \text{(S2-2)}$$

$$\left(\frac{2\pi f}{\gamma}\right)^2 = [H_{X\parallel}^R - \delta H_{X\parallel}^R\left(\frac{L}{R}\right)][H_{Y\parallel}^R - \delta H_{Y\parallel}^R(L/R)] \quad \text{(S3)}$$

$$H_{X\parallel}^R = H_r + 2H_{4//} + H_{2//}; H_{Y\parallel}^R = H_r + 4\pi M_{eff} + 2H_{4//}$$

$$\delta H_{X\parallel}^R\left(\frac{L}{R}\right) = 8.6 * \delta H^R\frac{L}{R}; \delta H_{Y\parallel}^R\left(\frac{L}{R}\right) = 4\pi\delta M_S^{\parallel}\left|\frac{L}{R}\right| + 372.1 * \delta H^R\frac{L}{R}$$

$$\left(\frac{2\pi f}{\gamma}\right)^2 = [H_{X\perp}^R - \delta H_{X\perp}^R\left(\frac{L}{R}\right)][H_{Y\perp}^R - \delta H_{Y\perp}^R(L/R)] \quad \text{(S4)}$$

$$H_{X\perp}^R = H_r - 4\pi M_{eff} * f_X^2\left(\frac{L}{R}\right) + 2H_{4\perp} * f_X^4\left(\frac{L}{R}\right) + H_{4//} * f_X^{4\parallel}\left(\frac{L}{R}\right)_+ H_{2//}$$

$$H_{Y\perp}^R = H_r + \left(H_{4\perp} - H_{4\parallel} - 4\pi M_{eff}\right) * f_Y^2\left(\frac{L}{R}\right) + (H_{4\perp} + H_{4\parallel}) * f_Y^4\left(\frac{L}{R}\right)$$

$$f_X^2\left(\frac{L}{R}\right) = \frac{1}{2}\left(1 + \frac{R}{L}sin\frac{L}{R}\right)$$

$$f_Y^2\left(\frac{L}{R}\right) = \frac{R}{L}sin\frac{L}{R}$$

$$f_X^4\left(\frac{L}{R}\right) = \frac{1}{2}\left(\frac{3}{4} + \frac{R}{L}sin\frac{L}{R} + \frac{1}{42}\frac{R}{L}sin\frac{2L}{R}\right)$$

$$f_Y^4\left(\frac{L}{R}\right) = \frac{R}{2L}sin\frac{2L}{R}$$

$$f_X^{4\parallel}\left(\frac{L}{R}\right) = \frac{3}{4} - \frac{R}{L}sin\frac{L}{R} + \frac{1}{42}\frac{R}{L}sin\frac{2L}{R}$$

$$\delta H_{Y\perp}^R\left(\frac{L}{R}\right) = \left(_{293.2} * \delta H^R\frac{L}{R} + 4\pi\delta M_S^{\perp}\left|\frac{L}{R}\right|\right) * f_Y^2\left(\frac{L}{R}\right) - 79.0 * \delta H^R\frac{L}{R} * f_Y^2\left(\frac{L}{R}\right)$$

$$\delta H_{X\perp}^{R}\left(\frac{L}{R}\right) = \left(\frac{}{370.5} * \delta H^{R}\frac{L}{R} + 4\pi\delta M_{S}^{\perp}\left|\frac{L}{R}\right|\right) * f_{X}^{2}\left(\frac{L}{R}\right) - 156.3 * \delta H^{R}\frac{L}{R} * f_{X}^{4}\left(\frac{L}{R}\right) -$$

$$0.8 * \delta H^{R}\frac{L}{R} * f_{X}^{4\parallel}\left(\frac{L}{R}\right) - 7 * \delta H^{R}\frac{L}{R}$$

$$\delta H^{R} = -0.359;\ \delta M_{S}^{\perp} = 97.05;\ \delta M_{S}^{\parallel} = 27.53$$

the magnetic dragging function for the in-plane condition is given by

$$\Xi = \cos\left(\phi - \phi_{H}\right) - \sin\left(\phi - \phi_{H}\right) * \frac{\frac{\partial}{\partial\phi}\left(H_{X\parallel}H_{Y\parallel}\right)}{\left(H_{X\parallel} + H_{Y\parallel}\right)H_{X\parallel}} \tag{S5}$$

$$H_{X\parallel} = H_{\mathrm{r}}\cos(\phi - \phi_{H}) + 2H_{4\ //}\cos 4\phi + H_{2\ //}\cos 2\phi; \tag{S5-1}$$

$$H_{Y\parallel} = H_{\mathrm{r}}\cos(\phi - \phi_{H}) + 4\pi\mathrm{M}_{\mathrm{eff}} + \frac{1}{2}H_{4\ //}\left(3 + \cos 4\phi\right) - H_{2\ //}\sin^{2}\phi \tag{S5-2}$$

The inhomogeneous broadening induced linewidth can be expressed as

$$\Delta H_{4\pi M_{eff}} = \left|\frac{H_{X\parallel}/\left(H_{X\parallel} + H_{Y\parallel}\right)}{\Xi}\right|\delta(4\pi M_{eff}) \tag{S6}$$

$$\Delta H_{\phi} = H_{r}\left|\frac{\sin\left(\phi - \phi_{H}\right) + \cos(\phi - \phi_{H}) * \frac{\frac{\partial}{\partial\phi}\left(H_{X\parallel}H_{Y\parallel}\right)}{\left(H_{X\parallel} + H_{Y\parallel}\right)H_{X\parallel}}}{\Xi}\right|\delta\phi \tag{S7}$$

the magnetic dragging function for the out-of-plane condition is given by

$$\Xi = \cos\left(\theta - \theta_{H}\right) - \sin\left(\theta - \theta_{H}\right) * \frac{\frac{\partial}{\partial\theta}\left(H_{X\perp}H_{Y\perp}\right)}{\left(H_{X\perp} + H_{Y\perp}\right)H_{Y\perp}} \tag{S8}$$

$$H_{X\perp} = H_{\mathrm{r}}\cos\left(\theta - \theta_{H}\right) - 4\pi M_{eff} * \cos^{2}\theta + 2H_{4\perp} * \cos^{4}\theta + H_{4\ //} *$$

$$\frac{1}{4}(7 - 6\cos^{2}\theta - \cos 2\theta)\sin^{2}\theta_{+}H_{2\ //} \tag{S8-1}$$

$$H_{Y\perp} = H_{\mathrm{r}}\cos\left(\theta - \theta_{H}\right) + \left(H_{4\perp} - H_{4\parallel} - 4\pi M_{eff}\right) * \cos 2\theta + \left(H_{4\perp} + H_{4\parallel}\right) * \cos 4\theta \tag{S8-2}$$

$$\Delta H_{4\pi M_{eff}} = \left|\frac{\left(-cos2\theta * H_{X\perp} - cos^2\theta H_{Y\perp}\right)/\left(H_{X\perp} + H_{Y\perp}\right) + sin\theta cos\theta \dfrac{\dfrac{\partial}{\partial\theta}\left(H_{X\perp} H_{Y\perp}\right)}{\left(H_{X\perp} + H_{Y\perp}\right) H_{Y\perp}}}{\Xi}\right| \delta(4\pi M_{eff})$$

(S9)

$$\Delta H_{\theta} = H_r \left|\frac{\sin\left(\theta - \theta_H\right) + cos\left(\theta - \theta_H\right) * \dfrac{\dfrac{\partial}{\partial\theta}\left(H_{X\perp} H_{Y\perp}\right)}{\left(H_{X\perp} + H_{Y\perp}\right) H_{Y\perp}}}{\Xi}\right| \delta\theta$$

(S10)